

Cite this: *Environ. Sci.: Nano*, 2024, **11**, 3816

# Atmospheric emissions of Ti-containing nanoparticles from industrial activities in China†

Qiuting Yang,<sup>ab</sup> Lili Yang,<sup>ab</sup> Changzhi Chen,<sup>bc</sup> Jianghui Yun,<sup>ab</sup>  
Chenyan Zhao<sup>bc</sup> and Guorui Liu \*<sup>abc</sup>

Inhalation of exogenous Ti-containing nanoparticles (NPs) can have adverse effects on human health. However, few studies have considered industrial emissions, which contribute significantly to atmospheric levels of Ti-containing NPs. In this study, we quantified Ti-containing NP emissions in samples of fine particulate matter (particle sizes: 40–120 nm) collected from 132 full-scale industrial plants. Coal-fired power plants emitted the highest particle number concentrations of Ti-containing NPs ( $1.7 \times 10^{10}$  particles per g), followed by solid waste incineration ( $7.7 \times 10^9$  particles per g) and blast furnace pig iron steelmaking ( $5.5 \times 10^9$  particles per g); coking plants and iron-ore sintering were also significant contributors to Ti-containing NPs emissions. Collectively, these five sources accounted for 99.9% of the annual atmospheric emissions of Ti-containing NPs from 13 industrial sectors in China (total  $\approx 9.8 \times 10^{22}$  particles). Moreover, these industrial emissions increased the atmospheric concentration of Ti-containing NPs by  $1.7 \times 10^7$  particles per  $m^3$ , therefore leading to the general population's lifetime average daily dose (LADD) of inhaled Ti-containing NPs being  $2.4 \times 10^6$  particles per day per kg. The findings presented herein highlight the importance of assessing NP emissions and advancing sustainable global industrial development.

Received 21st April 2024,  
Accepted 25th July 2024

DOI: 10.1039/d4en00347k

rsc.li/es-nano

## Environmental significance

Exogenous anatase TiO<sub>2</sub>-NPs have been detected in human cerebrospinal fluids. It has been reported that TiO<sub>2</sub>-NPs may not penetrate the skin to reach other tissues, but rather, they likely enter *via* the lungs and migrate to the brain or circulatory system, whereby they can reach other organs (*e.g.*, kidney, liver). *In vitro* studies of the cytotoxicity of TiO<sub>2</sub>-NPs in human cells indicate their potential to induce genetic toxicity, DNA damage, oxidative stress, inflammatory responses, or endoplasmic reticulum stress in cells and tissues. TiO<sub>2</sub>-NPs can also be hazardous to the cardiovascular system, *e.g.*, by causing or exacerbating systemic inflammation, endothelial dysfunction, lipid metabolism disorders, and atherosclerosis. Industrial activities are a cornerstone of human production and development. Despite the implementation of advanced pollution control measures, widespread industrial activities inevitably release fine particulate matter (PM) and toxic substances into the atmosphere, leading to adverse effects on the global environment and human health. Therefore, it is important to assess the emissions of Ti-containing NPs (*e.g.*, TiO<sub>2</sub>-NPs) from various industrial activities and identify the primary contributor.

## 1. Introduction

Industrial activities are a cornerstone of human production and development. Despite the implementation of advanced pollution control measures, widespread industrial activities inevitably release fine particulate matter (PM) and toxic substances into the atmosphere, leading to adverse effects on the global environment and human health.<sup>1–7</sup> It has been demonstrated that inhaling

fine PM can cause cardiovascular damage upon entering the bloodstream.<sup>8</sup> Additionally, exogenous PM can breach the blood–brain barrier to enter brain tissue.<sup>9</sup> The most significant and abundant components in fine PM are nanoparticles (NPs).<sup>10,11</sup> Exogenous anatase TiO<sub>2</sub>-NPs have been detected in human cerebrospinal fluids. It has been reported<sup>12</sup> that TiO<sub>2</sub>-NPs may not penetrate the skin to reach other tissues, but rather, they likely enter *via* the lungs and migrate to the brain or circulatory system, whereby they can reach other organs (*e.g.*, kidney, liver). *In vitro* studies of the cytotoxicity of TiO<sub>2</sub>-NPs in human cells indicate their potential to induce genetic toxicity,<sup>13</sup> DNA damage,<sup>13,14</sup> oxidative stress, inflammatory responses,<sup>15</sup> or endoplasmic reticulum stress<sup>16</sup> in cells and tissues. TiO<sub>2</sub>-NPs can also be hazardous to the cardiovascular system, *e.g.*, by causing or exacerbating systemic inflammation, endothelial dysfunction, lipid metabolism disorders, and atherosclerosis.<sup>17</sup>

<sup>a</sup> State Key Laboratory of Environmental Chemistry and Ecotoxicology, Research Center for Eco-Environmental Sciences, Chinese Academy of Sciences, P.O. Box 2871, Beijing, 100085, China. E-mail: grliu@rcees.ac.cn

<sup>b</sup> University of Chinese Academy of Sciences (UCAS), Beijing, 100049, China

<sup>c</sup> School of Environment, Hangzhou Institute for Advanced Study, UCAS, Hangzhou, 310024, China

† Electronic supplementary information (ESI) available. See DOI: <https://doi.org/10.1039/d4en00347k>



The toxicity of NPs depends primarily on their particle size and particle number concentration (PNC),<sup>18</sup> rather than their mass concentration. Similarly, toxicological and epidemiological studies<sup>19,20</sup> indicate that PNCs of ultrafine particles may exhibit more accurate correlations with health endpoints than their mass concentrations. To date, several studies<sup>21–23</sup> have determined the PNCs of Ti-containing NPs in environmental media, particularly in water environments. Relatively few studies have examined the emission sources of TiO<sub>2</sub> NPs. One study,<sup>24</sup> however, quantified and characterized the release of TiO<sub>2</sub> NPs from paint and stain under natural weathering scenarios, reporting concentrations of  $6.8 \times 10^{15}$  NPs per kg-paint and  $2.9 \times 10^{13}$  NPs per kg-stain. However, few studies<sup>25,26</sup> have investigated Ti-containing NPs originating from industrial production activities, which are considered the primary source of these NPs. Currently, there is a lack of comprehensive quantitative information about the PNC of Ti-containing NPs emitted from industrial activities. Wu *et al.*<sup>25</sup> determined that Ti-containing NPs are the main metal-NPs in coal fly ash emissions from coal-fired power plants, with concentrations ranging from  $2.5 \times 10^{10}$  to  $1.7 \times 10^{11}$  particles per g. Thus, it is crucial to evaluate Ti-containing NP emissions from various industrial activities. However, there is limited information available regarding atmospheric emissions of Ti-containing NPs from different industries, resulting in insufficient understanding of the health risks to the general population in China who may inhale those Ti-containing NPs. Addressing these knowledge gaps is vital for sustainable global industrial development.

It is difficult to compile a comprehensive emissions inventory because there is limited monitoring data from many industrial plants releasing Ti-containing NPs into the atmosphere. In this study, we collected field samples from 132 full-scale plants across 13 industrial sectors, culminating in one of the largest sample sizes in such research to date. Fine PM samples were collected during industrial production processes, and the particle size distribution (PSD) characteristics of Ti-containing NPs were analyzed. The Ti-containing NP concentrations were quantified using single particle inductively coupled plasma time of flight mass spectrometry (SP-ICP-TOF-MS), and emission factors (EF) were derived for each industrial category. The atmospheric emissions of Ti-containing NPs in mainland China were estimated, and their spatial distributions were mapped (nationally) based on the computed EFs and industrial production activities. We also conducted a comparative analysis of Ti-containing NP emissions from various industrial sectors across different provinces in China. This is crucial to identify and prioritize sources for developing effective control strategies. This research provides practical insights for promoting sustainable industrial development worldwide.

## 2. Methods

### 2.1 Sample collection

We collect fine PM from 132 industrial production sites spanning 13 source categories.<sup>27</sup> This collection was conducted according to modification of the stationary source sampling methods.<sup>28,29</sup> Details about the sampling sites and industrial

PM samples are provided in Fig. S1 and Table S1,<sup>†</sup> respectively. For each industrial source, samples were collected from at least five production facilities. For coal-fired power plants (CFPPs), waste incineration (WI) and other pollution sources closely associated with production and daily life, samples were gathered from at least twelve factories each. The sampling sites was at the outlet of the bag filter, marking the end of each production cycle. Each sample comprised a composite meticulously obtained through sampling at various time points. The samples were then mixed to ensure representativeness and to reflect the overall production status during the three-day collection period. To maintain sample integrity, they were promptly transferred to the laboratory for analysis.

### 2.2 Sample pretreatment

The 132 industrial PM samples were subjected to pretreatment using the extraction method described by Li *et al.*<sup>30</sup> and Tou *et al.*<sup>31</sup> These studies investigated the extraction of NPs in complex matrices, thus providing a valuable reference for the present investigation. The detailed pretreatment procedure is outlined as follows: 20 mg of industrial PM is weighed into a centrifuge tube, and 50 mL of Milli-Q water is added. Ultrasonication is carried out for 20 min (ultrasonic power = 285 W), while maintaining a temperature range of 15–25 °C using ice. The sedimentation method is then employed to separate NPs from large particles. Following Stokes' law, the optimal sedimentation time was determined to be 3.25 hours. Then, 1 mL of the supernatant of the extract (containing particles <1 μm in diameter) was collected and diluted with Milli-Q water (18.2 MΩ) to 50 mL (*i.e.*, a 50-fold dilution), and then further diluted to 500-fold, 5000-fold, and 50 000-fold. Before the next processing step, the samples underwent another round of ultrasonication.

### 2.3 Instrumental analysis and data processing

Single particle analysis of the 132 diluted industrial PM extracts was conducted using ICP-TOF-MS (TOFWERK icpTOF 2R/CETAC Iridia-Bio, Switzerland) to determine the PNC and PSD of Ti-containing NPs. Element-specific instrument sensitivities were calibrated using a multi-element solution mixture derived from a multi-element standard solution (0, 0.05, 0.1, 0.2, 0.5, 1 μg L<sup>-1</sup> for multi-element standard [QC21, NIST SRM, SPEX, USA] diluted in 1% HNO<sub>3</sub> from Beijing Institute of Chemical Reagents, China). The transport efficiency (TE) was determined *via* the known size approach, employing both AuNPs with a certified particle size of 40 nm (NCRM-Au 40 nm, National Centre for Nanoscience, China) in Milli-Q water and Au ionic standard solutions (GSB 04-1726-2004, National Nonferrous Metals and Electronic Materials Analysis and Testing Centre, China) of 0, 0.05, 0.1, 0.2, 0.5, and 1 μg L<sup>-1</sup> (diluted in 1% HNO<sub>3</sub>). The linear correlation coefficient (*R*) of the Ti ion standard curve was 0.999, and that of the Au ion standard curve was 0.997 (Fig. S2a and b,<sup>†</sup> respectively). Before analysis, the ICP-TOF-MS mass spectra were calibrated with a standard tuning solution based on <sup>23</sup>Na<sup>+</sup>, <sup>80</sup>Ar<sup>2+</sup>, and <sup>208</sup>Pb<sup>+</sup> target



isotopes using TofDaq Viewer (Version, TOFWERK). We applied the kinetic energy discrimination (KED) mode with a collision cell gas comprising 4.5% hydrogen gas in helium to mitigate multi-atomic interference. Each sample was collected over 180 s, and the pipeline was washed with Milli-Q water between each set of samples.

The particle detection threshold was calculated according to a compound Poisson distribution using the expression in eqn (1),

$$\text{threshold} = \text{mean} + (3.29\sigma + 2.71) \quad (1)$$

where mean and  $\sigma$  are the mean and standard deviation of the background signal in the analysis window of 100 data points.

The PNC of Ti-containing NPs was determined according to eqn (2):

$$\text{PNC (particles per g)} = \frac{\text{number of detected NPs} \times \text{dilution factor} \times \text{extraction volume}}{\text{acquisition time} \times \text{liquid flow} \times \text{transport efficiency} \times \text{industry PM mass}} \quad (2)$$

The data obtained from the single-particle experiments were analyzed using the time-of-flight single-particle investigator (TOF-SPI), which is an in-house LabVIEW program (LabVIEW 2018, National Instruments, TX, USA). Specifically, TOF-SPI is an open-source software written by Alexander Gundlach-Graham (<https://github.com/TOFMS-GG-Group>) and designed to process SP-ICP-TOF-MS data combined with liquid calibrations. In the data processing for this study, the element-specific backgrounds, critical values, absolute sensitivities, particle intensities, and elemental masses (in grams) per particle were all determined using this software.

#### 2.4 Estimation method and uncertainty

We used the EF methodology recommended by EMEP/EEA<sup>32</sup> and UNEP<sup>33</sup> to estimate the emission inventory of Ti-containing NPs from 13 industrial sectors. This prevalent estimation method involves integrating data about the occurrence of human activities (*i.e.*, activity data; AD) with coefficients that quantify emissions or removals per activity unit, *i.e.*, EFs, according to the expression, Emission = AD × EF.

Therefore, in this study:

$$\begin{aligned} \text{Ti-containing NP emission (particles)} \\ = \text{production (10}^3 \text{ t)} \textcircled{1} \times \text{EF} \end{aligned} \quad (3)$$

$$\begin{aligned} \text{EF of Ti-containing NPs (particles per t-product)} = & \text{pollution discharge coefficient} \left( \frac{10^3 \text{ g}}{\text{t of product}} \right) \\ & \times \text{PNC of Ti-containing NPs (particles per g)} \end{aligned} \quad (4)$$

$$\begin{aligned} \text{Pollution discharge coefficient} \left( \frac{10^3 \text{ g}}{\text{t product}} \right) = & \text{pollutant-producing coefficient} \left( \frac{10^3 \text{ g}}{\text{t product}} \right) \textcircled{2} \\ & \times \{1 - \text{average removal efficiency of end-treatment technology (\%)}\} \textcircled{3} \end{aligned} \quad (5)$$

Note that ① AD are sourced from official websites of international organizations and institutions, as well as the China Statistical Yearbook released by the National Bureau of Statistics of China (for details, see our previous research<sup>27</sup>); ② and ③ are specified by the Method and Coefficient Manual of Industrial Source Pollution Discharge Accounting<sup>34</sup> (see our previous research<sup>27</sup>).

To minimize variance in the PNCs of Ti-containing NPs among industrial PM samples within each industry, we used MS Excel data processing to remove extreme values and outliers (outside the  $\pm 1.5$  inter-quartile range). The zero value was also removed. The remaining PNC values were averaged to obtain the reported values.

In this study, the equation used to estimate the increase in Ti-containing NPs (particles per m<sup>3</sup>) in the atmosphere of

China caused by emissions from the 13 industrial sources was the following:

$$\begin{aligned} \text{Ti-containing NPs (particles per m}^3\text{)} \\ = \text{Ti-containing NP emission (particles)} \\ \div \text{national territorial area (km}^2\text{)} \textcircled{1} \\ \div \text{vertical height of PM}_{2.5}\text{(m)} \textcircled{2} \end{aligned} \quad (6)$$

Note that ① the national territorial area (km<sup>2</sup>) was determined from [https://www.stats.gov.cn/zt\\_18555/ztsj/hjtjzl/2006/202303/t20230302\\_1922569.html](https://www.stats.gov.cn/zt_18555/ztsj/hjtjzl/2006/202303/t20230302_1922569.html), and <https://www.cia.gov/the-world-factbook/countries/>; and ② Ti-containing NPs are mainly wrapped with PM<sub>2.5</sub>, where the vertical height<sup>35</sup> of PM<sub>2.5</sub> aggregation is considered to be the height of Ti-containing NPs released from industrial sources into the atmosphere and distributed vertically in the air.

The lifetime average daily dose of Ti-containing NPs through inhalation exposure (LADD<sub>inh</sub>) caused by 13 industrial sectors could be assessed by using the eqn (7). Parameters utilized in the eqn (7) are displayed in Table S2.†

$$\text{LADD}_{\text{inh}} = \frac{C \times \text{EF}}{\text{AT}} \times \left( \frac{\text{inhR}_{\text{child}} \times \text{ED}}{\text{BW}_{\text{child}}} + \frac{\text{inhR}_{\text{adult}} \times \text{ED}}{\text{BW}_{\text{adult}}} \right) \quad (7)$$



### 3. Results

#### 3.1 Particle number concentrations of Ti-containing NPs from industrial activities

Toxicological and epidemiological studies<sup>19,20</sup> have suggested that the PNCs of ultrafine particles may be more closely correlated with health endpoints than mass concentrations. However, few studies<sup>25</sup> have focused on Ti-containing NPs emitted during industrial production activities. Fig. 1 and Table S3† present the PNCs of Ti-containing NPs (particles per g) across 132 industrial activities and 13 types of industrial sources. Notably, the PNCs vary by one to two orders of magnitude across the 13 industrial sectors.

The PNCs of Ti-containing NPs emitted from 13 industrial sources ranged from  $10^7$  to  $10^{11}$  particles per g. Coal-fired power plants (CFPPs) emitted the highest PNC of Ti-containing NPs into the air (mean =  $1.7 \times 10^{10}$  particles per g; range =  $6.8 \times 10^8$  to  $4.2 \times 10^{11}$  particles per g; median =  $1.1 \times 10^{10}$  particles per g), consistent with Wu *et al.*'s findings<sup>25</sup> that Ti-containing NPs emitted from CFPP sources ranged in PNC from  $2.5 \times 10^{10}$  to  $1.7 \times 10^{11}$  particles per g. A possible reason is that  $\text{TiO}_2$  may be doped in some mineral components of coal.<sup>36</sup> Waste incineration is a vital method for disposing of both municipal solid waste (WI) and hazardous waste (HWI). However, this approach emits high concentrations of Ti-containing NPs into the air. Specifically, for the WI process: mean =  $7.7 \times 10^9$ , median =  $7.9 \times 10^9$ , range =  $9.7 \times 10^8$  to  $2.6 \times 10^{10}$  particles per g; and for the HWI process: mean =  $2.2 \times 10^9$ , median =  $2.8 \times 10^9$ , range =  $6.7 \times 10^8$  to  $4.2 \times 10^{10}$  particles per g. This may result from the extensive use of  $\text{TiO}_2$  (ref. 37–39) in pigments, coatings, food additives, pharmaceuticals, cosmetics, and electronic devices. High temperatures during waste incineration can

release Ti-containing NPs from these substances. Blast-furnace pig iron steelmaking (BFI) represents the initial steelmaking process, where iron ore is melted with coke in a blast furnace to produce pig iron or molten iron for steel refining. In contrast, electric-arc furnace steelmaking (EAF) uses scrap steel and electrical energy to facilitate steel recycling; this method is preferred in developed and rapidly developing countries. However, both of these steelmaking sectors emit relatively high PNCs of Ti-containing NPs, *i.e.*, BFI: mean =  $5.5 \times 10^9$  (range =  $1.1 \times 10^9$  to  $1.0 \times 10^{10}$  particles per g; median =  $5.3 \times 10^9$  particles per g); and EAF: mean =  $2.0 \times 10^9$  (range =  $2.7 \times 10^8$  to  $5.7 \times 10^9$  particles per g; median =  $5.7 \times 10^9$  particles per g). Co-disposing of solid waste in cement kilns (CK) involves introducing waste into the kiln, which yields cement clinker, while safely disposing of waste. However, this process inevitably emits significant PNCs of Ti-containing NPs into the atmosphere (mean =  $1.9 \times 10^9$ ; range =  $3.2 \times 10^8$  to  $1.9 \times 10^{10}$ ; median =  $8.2 \times 10^8$  particles per g). Based on these PNC values, we propose that it would be most effective to target the industrial sources that release the highest concentrations of Ti-containing NPs, *i.e.*, CFPP, WI, BFI, HWI, EAF, and CK, to achieve significant emissions reductions.

The industrial sectors, iron-ore sintering (IOS), secondary copper smelting (SCu), primary copper smelting (PCu), coking plants (COP), secondary aluminum smelting (SAI), secondary lead smelting (SPb), and secondary zinc smelting (SZn) emit relatively lower PNCs of Ti-containing NPs into the air (all approximately  $10^8$  particles per g). Specifically, the average PNCs from highest to lowest were COP ( $8.8 \times 10^8$ ), SCu ( $3.3 \times 10^8$ ), IOS ( $3.2 \times 10^8$ ), SAI ( $3.1 \times 10^8$ ), SPb ( $2.8 \times 10^8$ ), PCu ( $1.4 \times 10^8$ ), and SZn ( $1.3 \times 10^8$ ) particles per g.

The PNCs of Ti-containing NPs released from these industrial processes comprise important first-hand data from a large-scale investigation of industrial activities. In particular, sectors such as CFPP, WI, BFI, HWI, EAF, and CK emit high PNCs of Ti-containing NPs and are therefore crucial for understanding the current emission status of many industries in China.

#### 3.2 Particle size distributions of Ti-containing NPs from industrial activities

The samples obtained from the industry sources have complex compositions, including Ti-containing NPs (primarily  $\text{TiO}_2$  in two crystal forms: rutile and anatase). Thus, the PSD of Ti-containing NPs was calculated separately for rutile and anatase. The particle sizes of Ti-containing NPs were determined based on the mass and density of each type ( $\rho_{\text{rutile}} = 4.25 \text{ g cm}^{-3}$ ;  $\rho_{\text{anatase}} = 3.78 \text{ g cm}^{-3}$ ; mass values listed in Table S4†). The PSDs of Ti-containing NPs from various industrial sources were determined using SP-ICP-TOF-MS (Fig. 2 and S3†). The PSDs of Ti-containing NPs from similar industrial sources were consistent across different factories. However, variations were observed among different industrial sources. For example, BFI, IOS, WI, HWI, and EAF predominantly have particle sizes

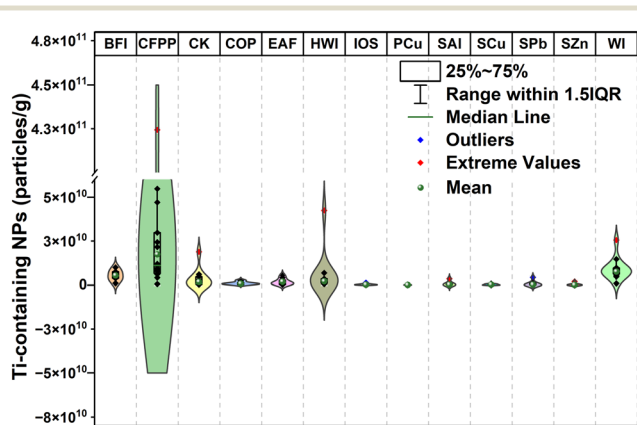


Fig. 1 PNCs of Ti-containing NPs (particles per g) released from 132 industrial activities. PNC = particle number concentration; NP = nanoparticle; PCu = primary copper smelting; SCu = secondary copper smelting; SAI = secondary aluminum smelting; SPb = secondary lead smelting; SZn = secondary zinc smelting; EAF = electric-arc furnace steelmaking; WI = municipal solid waste incineration; CK = cement kiln co-processing of solid waste; IOS = iron-ore sintering; COP = coking plant; HWI = hazardous-waste incineration; CFPP = coal-fired power plant; BFI = blast-furnace pig iron steelmaking.





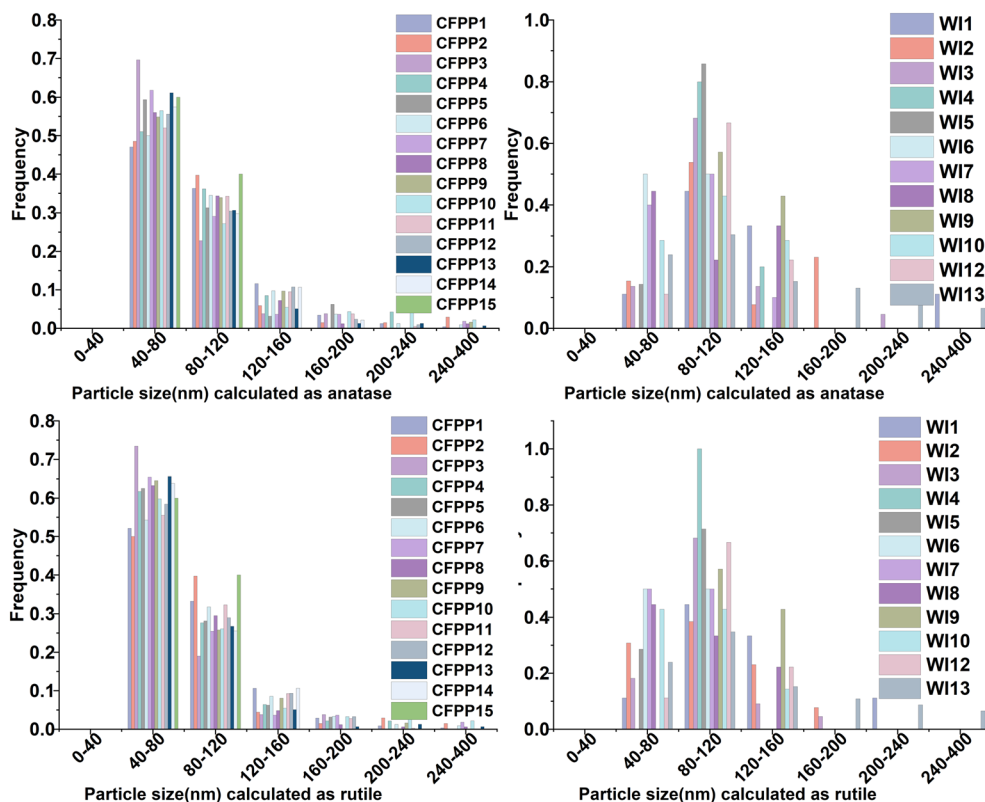


Fig. 2 PSDs of Ti-containing NPs released from CFPP and WI sources.

ranging from 80–120 nm, whereas CFPP, CK, COP, and SCu typically have particle sizes within the range of 40–80 nm. Overall, most particles are less than 120 nm in diameter.

For CFPP, assuming all Ti-containing NPs are anatase, the mean particle size ranged from 76.1 to 96.2 nm, with a median size between 70.6 and 83.5 nm and an overall range of 56.4 to 373.6 nm. This is consistent with Wu *et al.*'s findings<sup>25</sup> that the PSD for CFPP ranged from several nanometers to 200 nm. For WI, Ti-containing NPs (anatase) had mean particle sizes ranging from 83.8 to 127.3 nm and median sizes ranging from 82.0 to 115.3 nm, with all particles falling within the range of 70.6 to 418.2 nm. The mean, median, and overall range of particle sizes of anatase NPs emitted from the other industrial sources are presented in Table S5.† Anatase-NPs from BFI and HWI had the larger sizes: mean = 103.1–167.0 nm and 77.9–152.0 nm, and median = 91.6–174.3 nm and 77.9–160.0 nm, with overall particle sizes ranging from 68.9–488.6 nm and 70.4–318.8 nm, respectively.

Assuming all Ti-containing NPs are rutile leads to similar PSDs to those of anatase. The detailed mean, median, and overall range of particles size of rutile-NPs from the 13 industrial sources are presented in Table S6.† Herein, we discuss a few industrial sources as examples. For CFPP, the mean particle size of rutile-NPs ranged from 73.1 to 92.5 nm (median = 67.9 to 80.3 nm, range = 54.2 to 359.3 nm). In contrast, rutile-NPs from WI, BFI, and HWI were generally larger: mean = 80.6–137.2, 99.1–160.6, and 75.3–146.2 nm;

median = 78.8–110.8, 88.1–167.7, and 75.3–153.8 nm; and range = 67.9–402.2, 66.3–469.9, and 67.7–306.6 nm, respectively. In this study, SP-ICP-TOF-MS was employed to detect the PSDs of Ti-containing NPs emitted from industrial sources. The data obtained are comprehensive and important for increasing our understanding of emitted particle sizes.

### 3.3 Emissions factors of Ti-containing NPs from industrial activities

An EF reflects the average pollutant emission per unit of activity for a particular source. In this study, the EF was used to quantify the Ti-containing NPs emissions per ton of steel, copper, aluminum, lead, zinc, or disposed waste. It can also be used to assess emissions from coal-fired power generation of 1 terawatt hour (TW h). The EFs of Ti-containing NPs for various industrial sources were determined using eqn (4) (refer to the Method section).

The EFs for Ti-containing NPs across the 13 tested industrial sectors ranged from  $4.0 \times 10^9$  to  $1.7 \times 10^{13}$  particles per t-product (Fig. 3 and Table S7.†). The number of Ti-containing NPs emitted by the production of one ton of cement was the largest (up to  $1.7 \times 10^{12}$  particles), which indicates that advanced bag filter systems are necessary for CK sewage discharge control. The industrial sources with relatively high EFs of Ti-containing NPs included COP ( $3.9 \times 10^{11}$ ), BFI ( $2.5 \times 10^{11}$ ), EAF ( $2.1 \times 10^{11}$ ), SPb ( $1.9 \times 10^{11}$ ), SCu ( $1.6 \times 10^{11}$ ), and SAL ( $1.5 \times 10^{11}$  particles per t-product); the



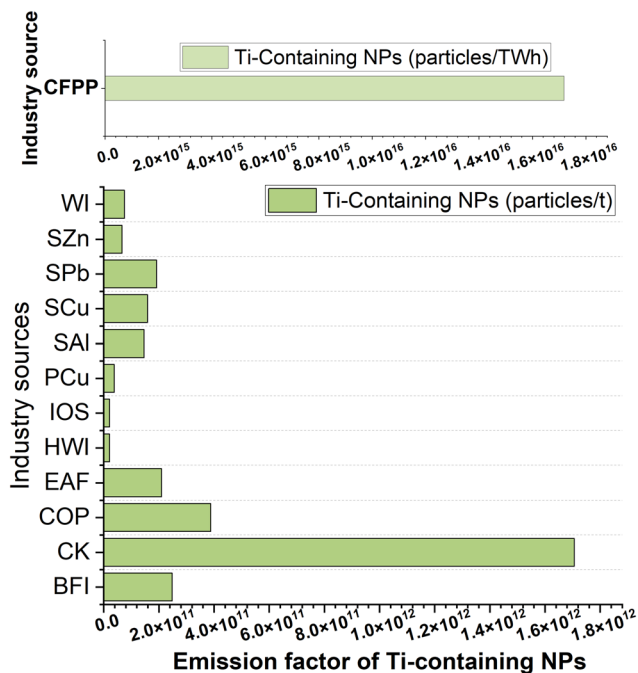


Fig. 3 Emission factors (particles per t or particles per TWh) of Ti-containing NPs for 13 industry sectors (note: the emission factor is the number of Ti-containing NPs emitted to the atmosphere by producing one ton of steel, copper, aluminum, lead, or zinc; disposing of one ton of waste; or producing one TWh).

industrial sources with relatively low EFs of Ti-containing NPs included WI ( $7.6 \times 10^{10}$  particles per t-disposal), SZn ( $6.7 \times 10^{10}$  particles per t-product), PCu ( $3.8 \times 10^{10}$  particles per t-product), HWI ( $2.2 \times 10^{10}$  particles per t-disposal), and IOS ( $2.1 \times 10^{10}$  particles per t-product). Notably, for every TW h generated by a CFPP,  $1.7 \times 10^{16}$  Ti-containing NPs are emitted into the atmosphere. These rarely-reported EFs provide a valuable reference for estimating Ti-containing NP emissions from industrial activities, both within China and worldwide.

### 3.4 Atmospheric emissions of Ti-containing NPs from industrial activities

China is a rapidly advancing industrialized nation that stands among the global leaders in terms of production output across 13 key industrial sectors. Moreover, China prides itself on possessing advanced technology and industrial production equipment that are on par with those of developed nations. Thus, examining the emissions of Ti-containing NPs from these 13 industrial activities in China can establish a valuable benchmark for developed nations to assess their own emissions. This evaluation also carries considerable weight in obtaining an initial estimation of the total global emissions of Ti-containing NPs.

It is crucial to elucidate the sources and quantities of Ti-containing NPs released from industrial activities to enable effective source management. We applied the EF methodology recommended by the European Monitoring and Evaluation Programme (EMEP) of the European Environment

Agency (EEA)<sup>32</sup> and the United Nations Environmental Program (UNEP)<sup>33</sup> to estimate the emission inventory. Atmospheric emissions of Ti-containing NPs from different industrial sources in China are presented in Fig. 4 and Table S8† (organized based on geographical distribution).

Our assessment of these 13 industrial sources indicated that annual atmospheric emissions of Ti-containing NPs in China reach approximately  $9.8 \times 10^{22}$  particles. This level of emissions could elevate the atmospheric concentration of Ti-containing NPs in China by  $1.7 \times 10^7$  particles per  $\text{m}^3$  (further details in the Method section). Such an escalation in concentration may lead to the general population's lifetime average daily dose (LADD) of inhaled Ti-containing NPs being  $2.4 \times 10^6$  particles per day per kg.

As shown in Fig. 4, CFPP ( $9.4 \times 10^{22}$  particles), CK ( $3.6 \times 10^{21}$  particles), BFI ( $2.2 \times 10^{20}$  particles), and COP ( $1.8 \times 10^{20}$  particles) are the top industrial contributors of Ti-containing NPs in China, collectively contributing 99.9% of the total annual atmospheric emissions of the 13 investigated industrial sources. Wide variations in Ti-containing NP emissions are observed across provinces for several industrial sources. For example, the disparities within SPb and HWI span up to four orders of magnitude; those for CFPP, PCu, SCu, and SAl reach three orders of magnitude, and those for COP, CK, EAF, WI, BFI, IOS, and SZn are up to two orders of magnitude.

We also roughly estimated the total global emissions of Ti-containing NPs from the 13 categories of industrial activities as  $1.8 \times 10^{23}$  particles (Table 1). China alone accounts for 54.2% of these emissions, which validates the broad importance of assessing the status of Ti-containing NP emissions in China. Similar to the case in China alone, CFPP ( $1.7 \times 10^{23}$  particles), CK ( $7.4 \times 10^{21}$  particles), BFI ( $3.3 \times 10^{20}$  particles), COP ( $2.7 \times 10^{20}$  particles), and EAF ( $1.2 \times 10^{20}$  particles) are the most significant industrial contributors of Ti-containing NPs globally. Collectively, these sectors contribute 99.9% of the total annual atmospheric emissions from the 13 investigated industrial sources. Thus, our first-hand findings confirm the important industrial sources of Ti-containing NPs both in China and globally.

Industrial development is vital for societal progress, especially in densely-populated countries like China, because it has a significant influence on national advancement and can improve living standards. Evaluating Ti-containing NP emissions through regional economic bodies helps with policy formulation and promotes emission reduction efforts. China's socioeconomic development is often evaluated by region, *i.e.*, eastern, central, western, and northeastern. The proportions of Ti-containing NP sources across different regions are shown in Fig. 5. The eastern regions are the top emitters, followed by the western and central regions. Therein, CFPP, WI, BFI, HWI, EAF, and CK are the sources with significant potential for effective reduction, and therefore, greater efforts are needed in these regions. In addition, because CFPP, CK, BFI, and COP are important industrial contributors, efforts should be concentrated in the



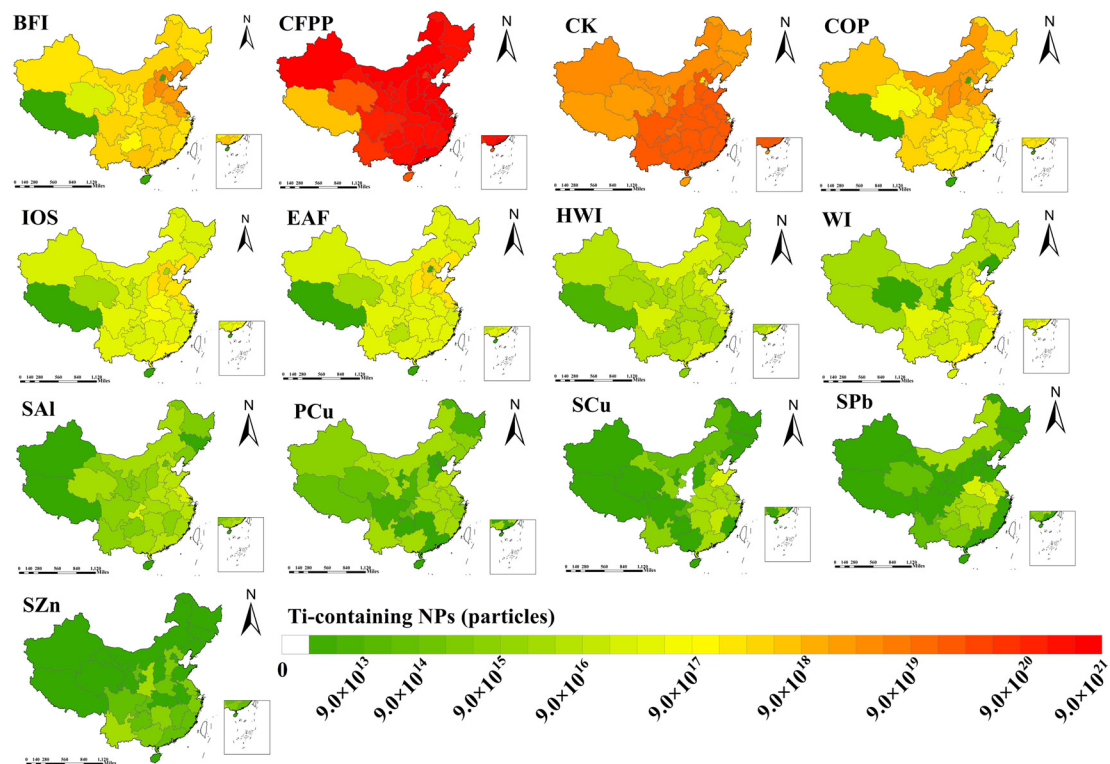


**Fig. 4** Total emissions (unit: particles) of Ti-containing NPs from thirteen industrial sources (the map is based on free vector data sourced from the “Database of National Catalogue Service for Geographic Information [GS (2020)4619]” (<https://www.resdc.cn/DOI/doi.aspx?DOIid=122>) and created using ArcGIS software). PCu = primary copper smelting; SCu = secondary copper smelting; SAl = secondary aluminum smelting; SPb = secondary lead smelting; SZn = secondary zinc smelting; EAF = electric-arc furnace steelmaking; WI = municipal solid waste incineration; CK = cement kiln co-processing of solid waste; IOS = iron-ore sintering; COP = coking plant; HWI = hazardous-waste incineration; CFPP = coal-fired power plant; BFI = blast-furnace pig iron steelmaking.

corresponding high-emission regions. In terms of CFPP emissions, the eastern region is the largest contributor (41.9%), followed by the western (30.9%) and central regions (21.2%). Increased efforts toward emission reduction of CK sources in eastern, western, and central China are therefore required. In the case of BFI, the eastern region is the dominant emitter, contributing 51.8% of the Ti-containing NP emissions in China. For COP, the western region plays a pivotal role, contributing 35.4% of Ti-containing NP

emissions, while the central and eastern regions contribute 33.2% and 23.5%, respectively.

### 3.5 Sustainable development and prioritizing industrial sources for Ti-containing NP emissions reductions

China is a leading industrial powerhouse with advanced technology, and therefore, it is pivotal to evaluate Ti-containing NP emissions from its main industrial sources. This evaluation

**Table 1** Industrial activity data and Ti-containing NPs emissions (units: particles) of 13 industrial sectors in China and globally

Industry	China production (thousand tons)	Global production (thousand tons)	Ti-containing NPs emission in China	Ti-containing NPs emission global
BFI	883 800	1 345 200	$2.2 \times 10^{20}$	$3.3 \times 10^{20}$
CFPP (TWh)	5468	10 041	$9.4 \times 10^{22}$	$1.7 \times 10^{23}$
CK	2 129 512	4 360 000	$3.6 \times 10^{21}$	$7.4 \times 10^{21}$
COP	471 161	683 000	$1.8 \times 10^{20}$	$2.6 \times 10^{20}$
EAF	118 641	556 748	$2.5 \times 10^{19}$	$1.2 \times 10^{20}$
HWI	84 612	1 175 219	$1.8 \times 10^{18}$	$2.5 \times 10^{19}$
IOS	1 105 517	2 560 000	$2.3 \times 10^{19}$	$5.4 \times 10^{19}$
PCu	6614	22 000	$2.5 \times 10^{17}$	$8.4 \times 10^{17}$
SAl	5504	74 700	$8.0 \times 10^{17}$	$1.1 \times 10^{19}$
SCu	2301	18 900	$3.7 \times 10^{17}$	$3.0 \times 10^{18}$
SPb	2198	6670	$4.2 \times 10^{17}$	$1.3 \times 10^{18}$
SZn	659	13 800	$4.4 \times 10^{16}$	$9.2 \times 10^{17}$
WI	117 892	271 960	$8.9 \times 10^{18}$	$2.1 \times 10^{19}$



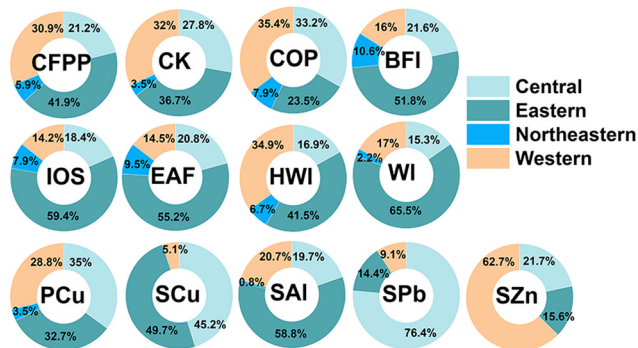


**Fig. 5** Proportions of Ti-containing NP emissions by industrial source in the four economic regions of China. PCu = primary copper smelting; SCu = secondary copper smelting; SAI = secondary aluminum smelting; SPb = secondary lead smelting; SZn = secondary zinc smelting; EAF = electric-arc furnace steelmaking; WI = municipal solid waste incineration; CK = cement kiln co-processing of solid waste; IOS = iron-ore sintering; COP = coking plant; HWI = hazardous-waste incineration; CFPP = coal-fired power plant; BFI = blast-furnace pig iron steelmaking.

can inform developed nations about their emissions to promote and guide global industrial sustainability. Emissions of Ti-

containing NPs differ significantly (by one to two orders of magnitude) among Chinese provinces. We identified nine provinces with the highest Ti-containing NP emissions and assessed specific industrial sector contributions therein (Fig. 6), thereby providing crucial insights for emission control strategies.

These nine provinces (Shandong, Inner Mongolia, Jiangsu, Guangdong, Xinjiang, Shanxi, Hebei, Anhui, and Henan) collectively accounted for  $5.7 \times 10^{22}$  particles of Ti-containing NPs (Fig. 6), corresponding to 58.3% of the total emissions from the 31 provinces in mainland China. Shandong leads with annual Ti-containing NP emissions of  $9.1 \times 10^{21}$  particles, followed by Inner Mongolia ( $8.4 \times 10^{21}$  particles) and Jiangsu ( $7.9 \times 10^{21}$  particles). Consequently, residents in these provinces may face elevated exposure risks. Focusing on these nine provinces when formulating Ti-containing NP emission reduction policies in China can lead to significant emissions reductions.

Among the nine provinces with the highest emissions of Ti-containing NPs (Fig. 6), four are situated in the eastern region, three in the central region, and two in the western region. This distribution is logical and can be attributed to the intense industrialization and rapid economic growth in

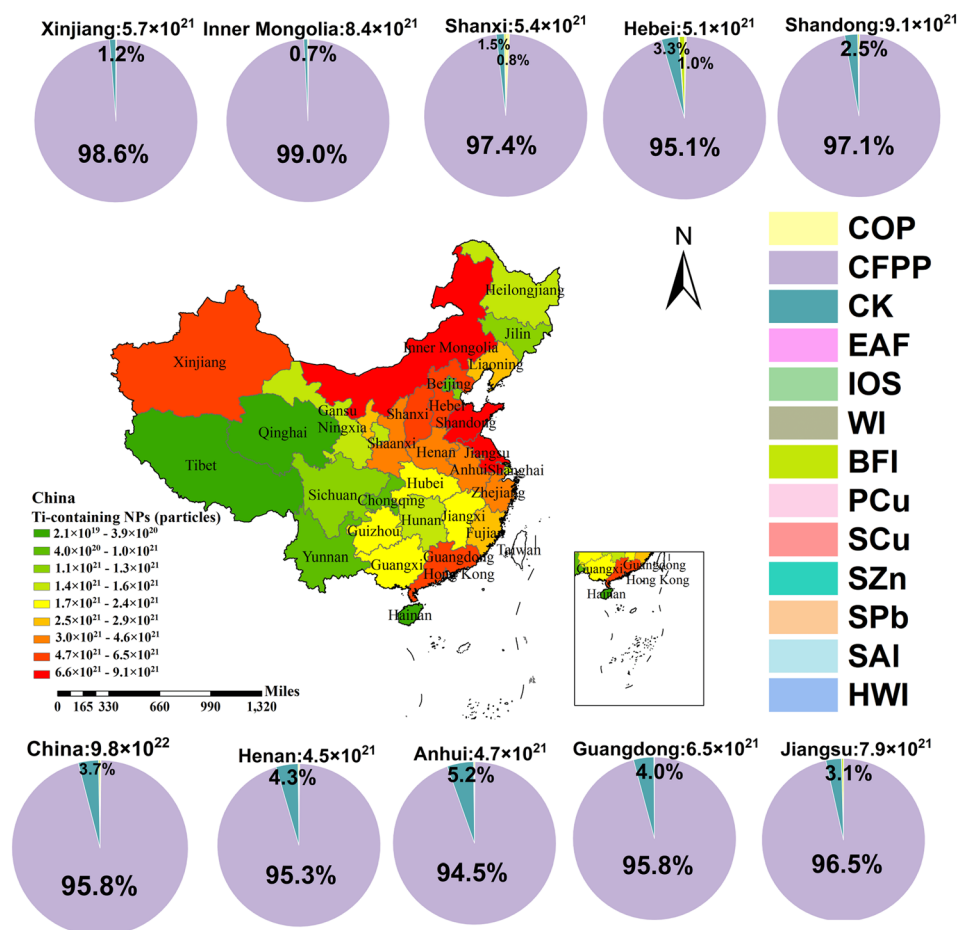


**Fig. 6** The distribution of Ti-containing NP emissions across the 31 provinces in mainland China and industrial sector-specific contributions in the nine provinces with the highest Ti-containing NP emissions.





the eastern and central regions of China. Significantly reducing emissions requires addressing two key industrial activities (*i.e.*, CFPP and CK) within these nine high-emission provinces. Additionally, provinces like Hebei should prioritize improvements in BFI, while Shanxi should focus on optimizing COP. Enhancing the efficiency of pollution control devices will mitigate health risks substantially for residents in provinces with high emissions.

## Data availability

All data in this study are contained in the manuscript and ESI.†

## Author contributions

Qiuting Yang conducted the production site field surveys, collected samples, designed the experiments, analyzed the data, and wrote the manuscript. Lili Yang contributed to sample collection and revised the manuscript. Changzhi Chen, Jianghui Yun, and Chenyan Zhao assisted in the sample collection. Guorui Liu conceptualized the study, conducted production site field surveys, wrote and revised the manuscript, and acquired funding.

## Conflicts of interest

The authors declare no competing interests.

## Acknowledgements

This work was supported by the Strategic Priority Research Program of the Chinese Academy of Sciences (Grant No. XDB07500400) and the National Natural Science Foundation of China (Grant No. 92143201 and 22076201). We thank Professors Chungang Yuan, DeAn Pan, Cheng Li, Pu Lv, Feihua Yang, Yinming Li, Jianxin Yang, Xiaojin Han, and Hua Yin for their help in sample collection.

## References

- 1 J. Lelieveld, *et al.*, The contribution of outdoor air pollution sources to premature mortality on a global scale, *Nature*, 2015, **525**, 367–371.
- 2 Z. A. Chafe, *et al.*, Household cooking with solid fuels contributes to ambient PM<sub>2.5</sub> air pollution and the burden of disease, *Environ. Health Perspect.*, 2014, **122**, 1314–1320.
- 3 C. Peng, *et al.*, Particulate Air Pollution and Fasting Blood Glucose in Nondiabetic Individuals: Associations and Epigenetic Mediation in the Normative Aging Study, 2000–2011, *Environ. Health Perspect.*, 2016, **124**, 1715–1721.
- 4 A. J. Cohen, *et al.*, Estimates and 25-year trends of the global burden of disease attributable to ambient air pollution: an analysis of data from the Global Burden of Diseases Study 2015, *Lancet*, 2017, **389**, 1907–1918.
- 5 M. H. Forouzanfar, *et al.*, Global, regional, and national comparative risk assessment of 79 behavioural, environmental and occupational, and metabolic risks or clusters of risks, 1990–2015: a systematic analysis for the Global Burden of Disease Study 2015, *Lancet*, 2016, **388**, 1659–1724.
- 6 Q. Wang, *et al.*, Short-term particulate matter contamination severely compromises insect antennal olfactory perception, *Nat. Commun.*, 2023, **14**, 4112.
- 7 T. Walser, *et al.*, Persistence of engineered nanoparticles in a municipal solid-waste incineration plant, *Nat. Nanotechnol.*, 2012, **7**, 520–524.
- 8 X. Liu, *et al.*, Serum apolipoprotein A-I depletion is causative to silica nanoparticles-induced cardiovascular damage, *Proc. Natl. Acad. Sci. U. S. A.*, 2021, **118**, 44.
- 9 Y. Qi, *et al.*, Passage of exogenous fine particles from the lung into the brain in humans and animals, *Proc. Natl. Acad. Sci. U. S. A.*, 2022, **119**, e2117083119.
- 10 J. Hofman, *et al.*, Ultrafine particles in four European urban environments: Results from a new continuous long-term monitoring network, *Atmos. Environ.*, 2016, **136**, 68–81.
- 11 H.-S. Kwon, *et al.*, Ultrafine particles: unique physicochemical properties relevant to health and disease, *Exp. Mol. Med.*, 2020, **52**, 318–328.
- 12 M. Shakeel, *et al.*, Toxicity of Nano-Titanium Dioxide (TiO<sub>2</sub>-NP) Through Various Routes of Exposure: a Review, *Biol. Trace Elem. Res.*, 2015, **172**, 1–36.
- 13 K. M. Pearce, *et al.*, Induction of Oxidative DNA Damage and Epithelial Mesenchymal Transitions in Small Airway Epithelial Cells Exposed to Cosmetic Aerosols, *Toxicol. Sci.*, 2020, **177**, 248–262.
- 14 S. Murugadoss, *et al.*, Agglomeration of titanium dioxide nanoparticles increases toxicological responses in vitro and in vivo, *Part. Fibre Toxicol.*, 2020, **17**, 10.
- 15 K. Becker, *et al.*, TiO<sub>2</sub> nanoparticles and bulk material stimulate human peripheral blood mononuclear cells, *Food Chem. Toxicol.*, 2014, **65**, 63–69.
- 16 S. A. Ferraro, *et al.*, Neurotoxicity mediated by oxidative stress caused by titanium dioxide nanoparticles in human neuroblastoma (SH-SY5Y) cells, *J. Trace Elem. Med. Biol.*, 2020, **57**, 126413.
- 17 T. Chen, *et al.*, Cardiovascular Effects of Pulmonary Exposure to Titanium Dioxide Nanoparticles in ApoE Knockout Mice, *J. Nanosci. Nanotechnol.*, 2013, **13**, 3214–3222.
- 18 A. Seaton, *et al.*, Nanoparticles, human health hazard and regulation, *J. R. Soc., Interface*, 2009, **7**, S119–S129.
- 19 R. Sinharay, *et al.*, Respiratory and cardiovascular responses to walking down a traffic-polluted road compared with walking in a traffic-free area in participants aged 60 years and older with chronic lung or heart disease and age-matched healthy controls: a randomised, crossover study, *Lancet*, 2018, **391**, 339–349.
- 20 A. Peters, *et al.*, Elevated particle number concentrations induce immediate changes in heart rate variability: a panel study in individuals with impaired glucose metabolism or diabetes, *Part. Fibre Toxicol.*, 2015, **12**, 7.
- 21 Y.-H. Hwang, *et al.*, Characterization of Ti-containing nanoparticles in the aquatic environment of the Tamsuei River Basin in northern Taiwan, *Sci. Total Environ.*, 2021, **797**, 149163.



- 22 S. Wu, *et al.*, Identification and quantification of titanium nanoparticles in surface water: A case study in Lake Taihu, China, *J. Hazard. Mater.*, 2020, **382**, 121045.
- 23 L. N. Rand, *et al.*, Quantifying Nanoparticle Associated Ti, Ce, Au, and Pd Occurrence in 35 U.S. Surface Waters, *ACS ES&T Water*, 2021, **1**, 2242–2250.
- 24 A. Azimzada, *et al.*, Single- and Multi-Element Quantification and Characterization of TiO<sub>2</sub> Nanoparticles Released From Outdoor Stains and Paints, *Front. Environ. Sci.*, 2020, **8**, 91.
- 25 J. Wu, *et al.*, Metal-Containing Nanoparticles in Low-Rank Coal-Derived Fly Ash from China: Characterization and Implications toward Human Lung Toxicity, *Environ. Sci. Technol.*, 2021, **55**, 6644–6654.
- 26 J. Wu, *et al.*, Vast emission of Fe- and Ti-containing nanoparticles from representative coal-fired power plants in China and environmental implications, *Sci. Total Environ.*, 2022, **838**, 156070.
- 27 Q. Yang, *et al.*, Atmospheric emissions of respirable quartz from industrial activities in China, *Nat. Sustain.*, 2024, DOI: [10.1038/s41893-024-01388-6](https://doi.org/10.1038/s41893-024-01388-6).
- 28 Ministry of Ecology and Environment of the People's Republic of China, Stationary source emission—Determination of mass concentration of particulate matter at low concentration—Manual gravimetric method, 2017.
- 29 European Standardization Committee, Stationary source emissions - Determination of the mass concentration of PCDDs/PCDFs and dioxin-like PCBs - Part 1: Sampling of PCDDs/PCDFs, 2006.
- 30 L. Li, *et al.*, Extraction Method Development for Quantitative Detection of Silver Nanoparticles in Environmental Soils and Sediments by Single Particle Inductively Coupled Plasma Mass Spectrometry, *Anal. Chem.*, 2019, **91**, 9442–9450.
- 31 F. Tou, *et al.*, Titanium and zinc-containing nanoparticles in estuarine sediments: Occurrence and their environmental implications, *Sci. Total Environ.*, 2021, **754**, 142388.
- 32 EMEP/EEA, Air pollutant emission inventory guidebook 2019-Technical guidance to prepare national emission inventories, 2019.
- 33 UNEP, Toolkit for identification and quantification of releases of dioxins, furans and other unintentional POPs under article 5 of the stockholm convention, 2013.
- 34 Ministry of Ecology and Environment of the People's Republic of China, Handbook of emission sources inventory survey, pollution discharge calculation methods, and coefficients, 2021.
- 35 C. Liu, *et al.*, Vertical distribution of PM(2.5) and interactions with the atmospheric boundary layer during the development stage of a heavy haze pollution event, *Sci. Total Environ.*, 2020, **704**, 135329.
- 36 J. C. van Dyk, Understanding the influence of acidic components (Si, Al, and Ti) on ash flow temperature of South African coal sources, *Miner. Eng.*, 2006, **19**, 280–286.
- 37 A. Weir, *et al.*, Titanium dioxide nanoparticles in food and personal care products, *Environ. Sci. Technol.*, 2012, **46**, 2242–2250.
- 38 A. P. Popov, *et al.*, TiO<sub>2</sub> nanoparticles as an effective UV-B radiation skin-protective compound in sunscreens, *J. Phys. D: Appl. Phys.*, 2005, **38**, 2564.
- 39 J. H. Braun, *et al.*, TiO<sub>2</sub> pigment technology: a review, *Prog. Org. Coat.*, 1992, **20**, 105–138.

